IGSHPA Research Track
Las Vegas, December 6-8, 2022

Experimental Performance Analysis of a Dual-Source Heat Pump Integrated with Thermal Energy Storage

Lingshi Wang **Xiaobing Liu** **Bo Shen** **Xiaoli Liu**
Anthony Gehl **Liang Shi** **Ming Qu**

ABSTRACT

To mitigate disturbances to the electric grid resulting from the growing penetration of intermittent and decentralized renewable generation, a dual-source (air source and ground source) heat pump (DSHP) integrated with thermal energy storage (TES) was developed. The DSHP can use either ambient air or the shallow subsurface of the ground to provide space heating or space cooling to the building as the conventional heat pump and produce hot/cold water for charging TES. Using dual sources (air and ground) can reduce the required size of the expensive ground heat exchangers while retaining high energy efficiency. During the off-peak period, the DSHP cools/heats the TES with low-cost electricity or overproduced renewable power. The stored cooling/heating energy in the TES is released during peak hours of the electric grid to meet the thermal demands of the building without consuming electricity to run the DSHP. A 2-ton (7 kW) prototype DSHP was developed and integrated with a 50-gallon (189 L) TES tank filled with a phase change material. Field tests were conducted to characterize the performance of the integrated system operating in various operation modes.

INTRODUCTION

Renewable power generated with wind, solar, and geothermal energy can replace part of the fossil fuel consumption for electricity generation and thus reduce greenhouse gas emissions. However, the mismatch between the intermittent renewable power supply and the fluctuating electric demand limits the high penetration of renewable energy (MIT, 2011; King et al., 2011). Thermal energy storage (TES) has attracted increasing attention to addressing this challenge (Calderon et al., 2020; Guelpa and Verda, 2019; Wang et al., 2020, 2022).

Buildings in the United States consume 75% of all US electricity and are responsible for 80% of peak electric demand (EIA, 2018). Among all power consumption in buildings, 40%–70% is for thermal loads, including space heating and cooling (Wang et al., 2020). Because heat pumps can provide space cooling, space heating, and water heating, integrating TES systems with heat pumps could shift or level the behind-the-meter electric demand of buildings. When integrating

Lingshi Wang is an R&D Associate Staff, Xiaobing Liu (liux2@ornl.gov), Bo Shen and Anthony C. Gehl are Senior R&D Staff, and Xiaoli Liu is a postdoc at Oak Ridge National Laboratory. Liang Shi is a Ph.D. candidate and Ming Qu is a Professor at Purdue University

TES with a heat pump, the TES can be charged using low-cost electricity to store cooling or heating energy during the off-peak period. The stored energy can be discharged during peak hours to meet the thermal demands of the building without consuming electricity to run the heat pump.

To prove the feasibility of integrating TES into the heat pump system for demand response, this study developed a 2-ton (7 kW) prototype dual-source (air source and ground source) heat pump (DSHP) integrated with a 50-gallon (189 L) TES tank filled with phase change materials (PCMs) for residential applications (i.e., single-family houses). This integrated system not only provides heating and cooling to a building but also produces hot/cold water for charging the TES. The addition of an air source allows the heat pump to extract heat from or reject heat to the ambient when the ambient air is at favorable temperatures for highly efficient operation. At other times, the heat pump will use the ground as its heat sink/source to retain high efficiency. Because the thermal load of the ground heat exchanger is reduced, the required size of the expensive ground heat exchangers can also be reduced. Thus, the system can be more economically competitive than conventional ground source heat pump systems while retaining high energy efficiency. Field tests were conducted to evaluate the performance of the DSHP operating in various operation modes. This paper presents the charging and discharging performance of the integrated TES and DSHP for cooling operation.

SYSTEM CONFIGURATION AND TEST FACILITY

A prototype DSHP was designed and built at the US Department of Energy's Oak Ridge National Laboratory (ORNL). As shown in Figure 1, the DSHP circulates the refrigerant through either of the two parallel source-side heat exchangers: a ground source tube-in-tube heat exchanger or an air source microchannel heat exchanger. On the load side, the DSHP also has two parallel heat exchangers: an indoor direct expansion (DX) coil for producing hot or cold air, and a brazed plate heat exchanger to produce hot or chilled water for storing energy in the TES. A four-way valve switches between cooling and heating operation modes. Two thermo-expansion valves control the exit superheat degrees of the air source and the ground source heat exchanger, respectively, when they are working as evaporators. An electronic expansion valve controls the superheat degree out of the brazed heat exchanger when producing chilled water to charge the TES. A liquid receiver and a suction line accumulator were installed at the liquid line and before the suction port of the compressor to buffer the refrigerant charge among multiple operation modes, including space cooling and heating, as well as cooling and heating energy storage, using ground or air source. Five motorized ball valves isolate unused heat exchangers and manage charging migration during mode transitions. Figure 1a shows the cooling mode operation of the DSHP system, and Figure 1b shows an integrated DSHP and TES system for a residential application.

Integrating a DSHP with a TES tank enables shifting electric demand for space heating/cooling from on-peak hours to off-peak hours of the electric grid. During the off-peak period, the DSHP can simultaneously or alternatively provide space heating/cooling and supplies heating/cooling energy to the TES. During the on-peak hours, the stored energy is discharged from the TES through a fan coil to heat or cool the building without consuming electricity to operate the DSHP. The integrated DSHP and TES can be operated in 14 different modes, as listed in Table 1.

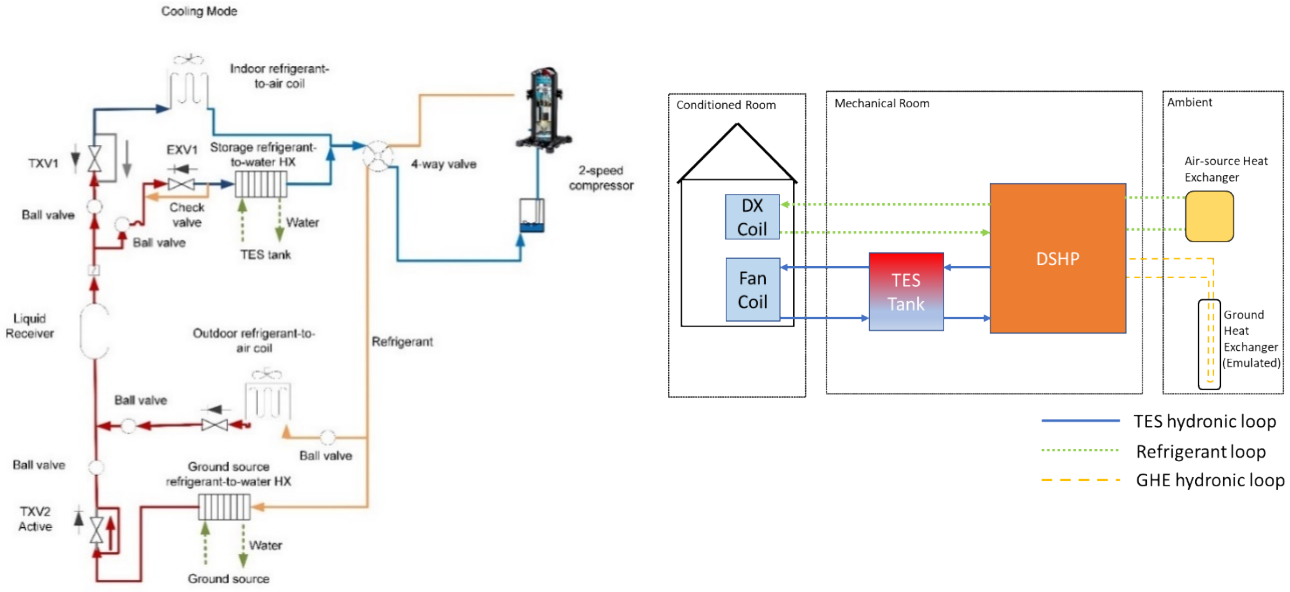

Figure 1 (a) Schematic of a DSHP in cooling mode, and (b) integration of a DSHP and TES in a residential application. EXV: electronic expansion valve; HX: heat exchanger; TXV: thermo-expansion valve

Table 1: Operating modes of the integrated DSHP and TES system

Mode	Source	Load	Performance
Heating	Ground	Space heating	Function tested
		Charging TES	Function tested
		Space heating and TES discharging	Function tested
	Air	Space heating	Function tested
		Charging TES	Function tested
		Space heating and TES discharging	Function tested
Cooling	Ground	Space cooling	Function tested
		Charging TES	Function tested (presented in this paper)
		Space cooling and TES discharging	Function tested
	Air	Space cooling	Function tested
		Charging TES	Function tested (presented in this paper)
		Space cooling and TES discharging	Function tested
TES discharge	Off	Space heating through fan coil unit	Function tested
		Space cooling through fan coil unit	Function tested (presented in this paper)

An experimental 2-ton (7 kW) DSHP integrated with a 50-gallon (189 L) TES tank filled with PCM was installed at ORNL's two-story Flexible Research Platform (FRP-2) at ORNL, as shown in Figure 2. ORNL's FRP-2 is a 3,200 ft^2 (297 m^2) 2-story building with 10 zones and a 12-ton (42 kW) distributed ground source heat pump system, which comprises 4 extended range water source heat pump (WSHP) units and a common water loop that connects the source side of the WSHP units. The FRP hosts a ground source emulator, which is a mechanical system that can maintain the supply water temperature of the common water loop at a user-specified temperature within the range of 45°F to 95°F (7°C to 35°C). A pump circulates water flow through all the WSHP units. One of the WSHP units was modified to be a DSHP with a 2-ton (7 kW) cooling capacity. An outdoor unit containing a microchannel heat exchanger and an axial

fan is connected to the WSHP to enable air-source operation. There are more than 500 various sensors installed in the FRP-2 to measure the temperature, pressure, and flow rates of air, water, and refrigerants of the heat pumps and other HVAC systems in the building. The specifications of the measurement instrumentations for the integrated DSHP and TES system are provided in Table 2.

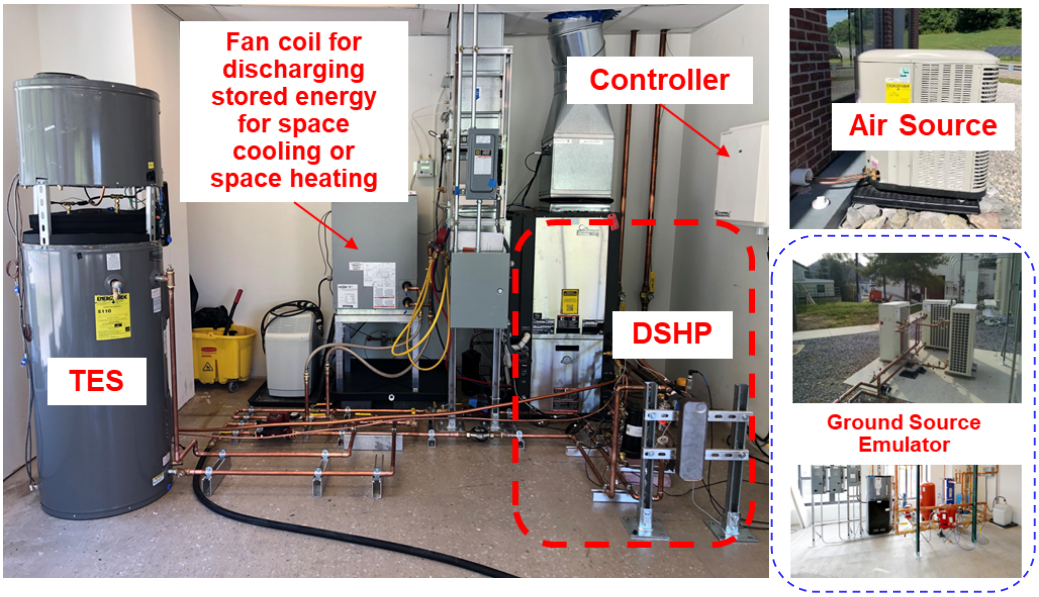

Figure 2 On-site photo of the developed DSHP and TES system

Table 2: Specifications of the measurement instrumentations

Measured property	Instrument	Range	Uncertainty
Water temperature	T-type thermocouple probes (Omega)	−270°C to 370°C	±0.5°C
Water flow rate	FTB4607 Long-Life Pulse Output Water Meters	0.22–20 GPM (0.83-75.7 LPM)	±1.5% of rate
Power	WNB-3Y-208-P Watt Node Pulse Electric Power Meter	0.375 Wh per pulse	±0.5% of reading
Air flow rate	Veltron DPT 2500-plus Differential Pressure and Flow Transmitter	0–1,760 CFM (0-2990 m^3/h)	±0.25% of the full scale
Air humidity and temperature	HMT330 Humidity and Temperature Transmitters	0%–100% relative humidity (RH), −40°C to 180°C	±(1.5 + 0.015 × reading) %RH, ±0.2°C

RESULTS AND DISCUSSIONS

A series of tests were conducted to verify the function of each of the 14 operation modes listed in Table 1. Key performance metrics were evaluated based on the measured data, including heating and cooling capacity, coefficient of

performance (COP), and supply air and water temperature. The charging and discharging performances for cooling with a 70°F (21.1°C) heat sink temperature (from an air source or ground source) are presented in this paper. In the tests presented here, water/ice was used as the PCM given its low cost and high thermal conductivity, as described in Table 3. Water was sealed in 48 aluminum tubes, which are 36 in. (91 cm) tall with a 2 in. (5 cm) diameter. These tubes were filled into the TES tank and occupied 52% of the tank volume. Antifreeze solution (30% propylene glycol in volume) was used to fill the remaining volume of the TES tank and transfer heat between the DSHP and the water in the tubes. The shortcoming of using water as a PCM is that its melting/freezing temperature is fixed at 32°F (0°C), so its solid-liquid phase change is only for storing cooling energy. This TES tank can also be used for sensible heat storage. Other PCMs can be used to store cooling or heating energy at a higher phase-changing temperature. Performance tests of the TES using other PCMs are reported by Wang et al. (2022).

Table 3: Physical properties of the PCM than can be added to the TES tank

PCM type	Composition	Latent heat	Freezing temperature	Melting temperature	Thermal conductivity (20°C)	Specific heat capacity	Density	Volumetric latent heat
		J/g	°C	°C	W/(m·°C)	kJ/(kg·°C)	g/cm^3	J/cm^3
Organic	Methyl laurate	176	3	5	0.15 (liquid), 0.23 (solid)	1.7	0.87	153
Inorganic	Water	334	0	0	0.6 (liquid), 2.2 (solid)	4.2	1	307

The COP of the DSHP was calculated with Eq. (1):

$$COP = \frac{\dot{Q}_{hydr} + \dot{Q}_{DX}}{W} \quad (1)$$

where $\dot{Q}_{hydr}$ is the cooling or heating energy from the plate heat exchanger for charging the TES, $\dot{Q}_{DX}$ is the cooling or heating energy provided by the DX coil, and W is the compressor power draw.

$\dot{Q}_{hydr}$ and $\dot{Q}_{DX}$ were calculated with Eqs. (2) and (3), respectively.

$$\dot{Q}_{hydr} = \dot{m}_w c_{p,w} \Delta T_{hydr} \quad (2)$$

$$\dot{Q}_{DX} = \dot{m}_a \Delta h_a \quad (3)$$

where $\dot{m}_w$ is the measured flow rate, $c_{p,w}$ is the specific heat (constant), and ΔT_{hydr} is the measured temperature difference between the inlet and outlet water at the plate heat exchanger; $\dot{m}_a$ is the measured flow rate, and Δh_a is the enthalpy difference between the supply air and return air at the DX coil. Enthalpy was calculated based on the measured temperature and humidity of the air.

The accumulated energy charged in/discharged from the TES (E_{TES}) was calculated with Eq. (4).

$$E_{TES} = \int \dot{Q}_{TES} dt \quad (4)$$

where t is time and $\dot{Q}_{TES}$ is the cooling or heating energy charged in/discharged from the TES, which was calculated with Eq. (5).

$$\dot{Q}_{TES} = \dot{m}_w c_{p,w} \Delta T_{tank} \quad (5)$$

where ΔT_{tank} is the temperature difference between the inlet and outlet of the tank, which are located at the top and bottom of the tank.

The state of charge (SOC) of the TES is defined as the ratio of the cumulative thermal energy charged into the TES to

the maximum thermal storage capacity of the TES, as expressed in Eq. (6),

$$SOC = \frac{E_{TES}}{Q_{TES,max}} \times 100\% \quad (6)$$

where $Q_{TES,max}$ is the maximum thermal storage capacity of the TES for cooling.

The state of discharge (SOD) is computed from Eq. (7).

$$SOD = 100\% - SOC \quad (7)$$

Figure 3 displays the charging performance of the TES tank in the DSHP system for cooling. As the charge of the TES tank started, the chilled antifreeze solution was supplied to the tank inlet at the bottom of the tank to store cooling energy inside the tank. Figure 3a shows that the tank inlet temperature first decreased from 51.6°F (10.9°C) to 21.3°F (-5.9°C) almost linearly. This process (from 11:59 to 12:11) was sensible cooling with a heat flow rate that varied from 5.17 to 1.46 kW (Figure 3b). The cooling COP dropped from 6 to 2.3 (Figure 3d) with the decrease in the tank inlet temperature. Since 12:11, the tank inlet temperature was maintained within a narrow range from 20.4°F to 21.7°F (-6.4°C to -5.8°C) with a cooling rate of 1.36–1.63 kW. This process was dominated by latent cooling with a cooling COP of approximately 2.13–2.44. Figure 3c shows that the antifreeze flow rate dropped in the same pattern as its temperature because of the increased viscosity of the antifreeze solution at lower temperatures. The state of charge in Figure 3b indicated that the TES tank took less than 4 h to be charged to 81% of its full capacity by the DSHP. The total cooling energy charged to the TES tank is 7.4 kWh, and the maximum storage capacity of the tank was 9 kWh when water was used as a PCM. For comparison, when only sensible cooling was stored in the 50-gallon (189 L) tank by cooling water from 51.6°F (10.9°C) to 32°F (0°C), 2.2 kWh of cooling energy can be stored. Thus, adding latent cooling of ice increases the cooling storage capacity by more than four times.

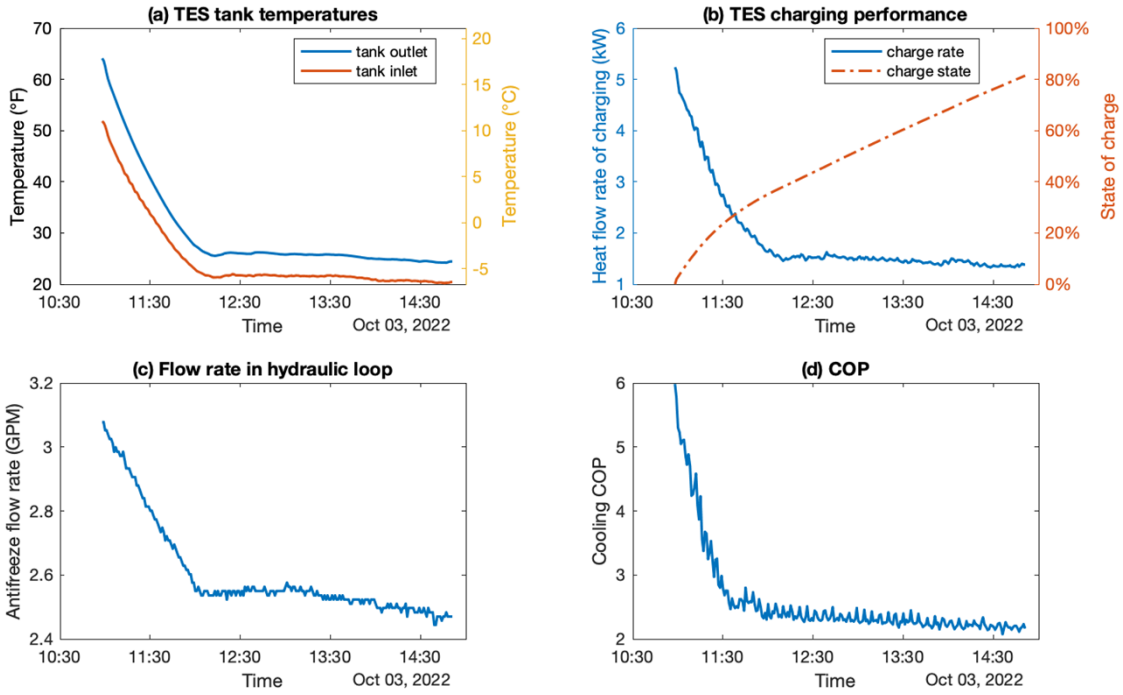

Figure 3 Cooling charge performance of the integrated DSHP and TES system running with an air source: (a) tank temperatures, (b) heat flow rate and state of charge, (c) flow rate of antifreeze, and (d) cooling COP.

Figure 4 presents the discharging performance of the TES tank for space cooling. As shown in Figure 4a, the TES tank provided chilled fluid at the outlet (at the bottom of the tank) with a temperature lower than 55°F (12.8°C) for approximately 2 h. The room temperature was maintained at the 75°F (23.9°C) set point with a fluctuation of around ±0.5°F (±0.3°C). During the process of (0) – (1) in the figure, from 15:38 to 16:12, the discharging rate (Figure 4b) dropped from 8.86 to 4.40 kW with an antifreeze flow rate of approximately 2.6 GPM (9.8 LPM) (Figure 4c). When the room temperature reached the set point, the TES discharging was suspended. The slope of the tank outlet (supply) temperature change was relatively small during this period, primarily because of the latent cooling capacity of the TES system. After the room temperature exceeded the upper limit of the temperature set point at 16:24, the TES tank discharged chilled water again until it reached a state of discharge of 81.2% at 17:49. The slope of the tank outlet temperature rise changed around 17:20 when most latent cooling was depleted (i.e., ice was melted in the tubes inside the tank). The higher slope at the process (2) – (3) in the figure indicates sensible cooling during this period. During a 2.2 h operation, the total cooling energy discharged from the tank was 7.98 kWh. The total discharged cooling was slightly higher than the total stored cooling because of the following two factors: (1) the tank temperature at the end of the discharge process was 3.45°F (1.9°C) higher than the starting temperature of the charging process, so more sensible cooling was released in the discharge process; and (2) the ice/frost cumulated on the surface of the plate heat exchanger and the hydronic piping during the charging process melted during the discharging process, which increased the cooling energy output. Overall, the roundtrip efficiency of the TES was nearly 1 with little heat loss.

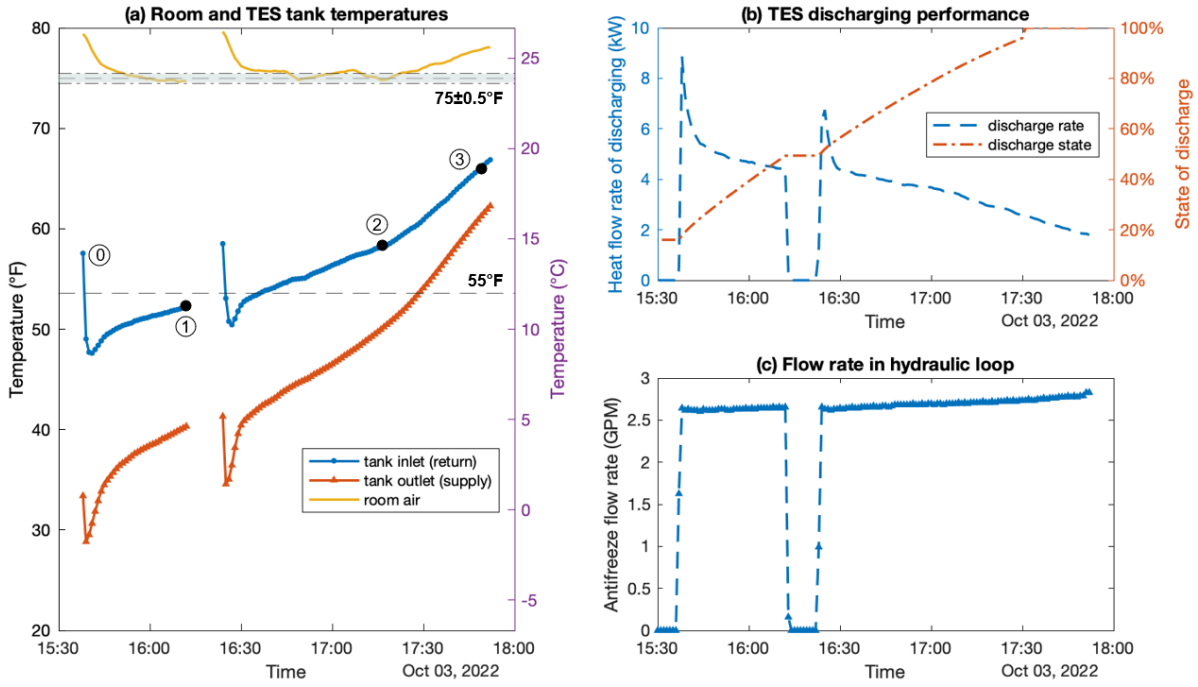

Figure 4 Discharging performance of a TES tank in the DSHP system: (a) room and tank temperatures, (b) heat flow rate and state of discharge, and (c) flow rate of antifreeze.

CONCLUSIONS AND FUTURE WORK

A 2-ton (7 kW) DSHP integrated with a TES that has 9 kWh thermal storage capacity was developed to condition room air and produce hot/cold water for charging TES either alternatively or simultaneously. The DSHP can use an air source

or a ground source (or both) depending on weather conditions. Field tests were conducted with the DSHP and TES system to evaluate its performance in various operation modes. The results presented in this paper indicate that the DSHP can cool the TES below the freezing point of water and make ice to store cooling energy. With the latent cooling of ice, the maximum storage capacity of the TES tank is 9.1 kWh, which is four times that of storing only sensible cooling in the 50-gallon (189 L) tank by cooling water from 51.55°F (10.9°C) to 32°F (0°C). It took 4 h for the DSHP to charge the TES to 81% of its full capacity using ambient air (ranging from 70°F (21.1°C) to 75°F (23.9°C)) as a heat source. During the ice-making process, the tank inlet temperature was maintained between 20.42°F and 21.65°F (-6.4°C and -5.8°C) with a heat transfer rate ranging from 1.36 to 1.63 kW and a cooling COP of approximately 2.13–2.44. The 7.4 kWh cooling energy stored in the TES tank was released in 2.2 h before the supply water temperature from the TES tank reached 55°F (12.8°C). Overall, the roundtrip efficiency of the TES was nearly 1 with little heat loss.

In future studies, the integrated DSHP and TES will be operated with automated control, either rule-based or model-predictive, to demonstrate the load-shifting performance of the system under real weather conditions in ORNL's FRP-**2**. Future studies will also include replacing the water in the aluminum tubes with an organic PCM, methyl laurate, which can be frozen at 37.4°F (3°C) and melted at 41°F (5°C). The higher freezing and melting temperature of methyl laurate may allow the heat pump to operate at a higher evaporating temperature and subsequently with a higher COP. However, methyl laurate has a much lower thermal conductivity than ice. Carbon fiber inserts will be added to the methyl laurate to increase heat transfer from the tube surface to and within the methyl laurate.

ACKNOWLEDGMENTS

This study was funded by the US Department of Energy (DOE) Office of Energy Efficiency and Renewable Energy, Geothermal Technologies Office. This manuscript has been authored by UT-Battelle, LLC, under contract DE-AC05-00OR22725 with the US Department of Energy (DOE). The US Government retains and the publisher, by accepting the article for publication, acknowledges that the US government retains a nonexclusive, paid-up, irrevocable, worldwide license to publish or reproduce the published form of this manuscript or allow others to do so, for the US government purposes. DOE will provide public access to these results of federally sponsored research in accordance with the DOE Public Access Plan (http://energy.gov/downloads/doe-public-access-plan).

REFERENCES

Calderóna, A., C. Barreneche, K. Hernández-Valle, E. Galindo, M. Segarra, and A. I. Fernández. 2020. *Where is Thermal Energy Storage (TES) research going? – A bibliometric analysis*. Solar Energy 200: 37–50.

Guelpa, E. and V. Verda. 2019). *Thermal energy storage in district heating and cooling systems: A review*. Applied Energy, 252: 113474.

King, J., T. Mousseau, and R. Zavadil. (2011). Eastern Wind Integration and Transmission Study. National Renewable Energy Laboratory, Golden, CO.

MIT (2011). The Future of the Electric Grid. Massachusetts Institute of Technology, Cambridge, MA.

U.S. Energy Information Administration (2018). Annual Energy Outlook 2018. Washington, DC. https://www.eia.gov/outlooks/aeo/2

Wang, L., Xiaobing Liu, Zhiyao Yang, Kyle R. Gluesenkamp. (2020). *Experimental study on a novel three-phase absorption thermal battery with high energy density applied to buildings*. Energy, 208:118311.

Wang, L., X. Liu, M. Qu, L. Shi, and X. Zhou. (2022). "*Experimental Evaluation of Thermal Storage Performance of a Dual-Purpose Underground Thermal Battery*." Proceedings of 2022 GRC Conference, August 28-30, Reno, Nevada